

Infrared-ellipsometry evidence of disorder-induced vibrational frequency shifts in hydrogenated-amorphous-silicon thin films

R. Ossikovski* and B. Drévilion

Laboratoire de Physique des Interfaces et des Couches Minces (UPR 258 du CNRS), Ecole Polytechnique, 91128 Palaiseau cedex, France

(Received 13 March 1995; revised manuscript received 15 July 1996)

In situ infrared ellipsometry is used systematically to study the thickness-dependent vibrational frequency shift of the Si-H stretching mode in plasma-deposited hydrogenated-amorphous-silicon thin films. The shift effect is shown to be dependent on the deposition conditions. After a detailed discussion of the possible physical origins of the frequency shift it is established that the latter is a result of the increased structural disorder at the film-substrate interface. A physical picture in terms of film-growth mechanisms is proposed and the role of hydrogen discussed. An analytical model based on the polarized medium theory enabled us to obtain the effective dynamical charges of the Si-H bond vibration in different bonding configurations. The values of the effective charges thus obtained are $(0.41 \pm 0.01)e$ and $(0.24 \pm 0.03)e$ (where e denotes the elemental charge) for the SiH and SiH₂ group vibrations, respectively. Highly sensitive infrared techniques are shown to be capable of probing the local structural order of the material, as in the case of Raman scattering spectroscopy. The results and conclusions presented in the following are expected to be helpful in our better understanding of the intimate link between vibrational and structural properties of *a*-Si:H. [S0163-1829(96)04740-6]

I. INTRODUCTION

The infrared (ir) vibrational spectroscopy studies of hydrogenated amorphous silicon (*a*-Si:H) have always been of great help to our basic understanding of silicon-hydrogen bonding in this material, as well as of the key role played by hydrogen in determining *a*-Si:H properties. Now it is well established that owing to its high mobility and reactivity H passivates the electronic defect states of *a*-Si:H and assists the relaxation of the overcoordinated *a*-Si network, improving in this way both the electronic and structural properties of the material. The pioneering ir-absorption studies have shown that H in *a*-Si:H is bonded in the form of three groups SiH_{*n*}, with *n*=1, 2, and 3.¹ Further investigations showed that most of the hydrogen in device-quality material exists as SiH groups homogeneously distributed in the bulk and displaying a dominant feature centered at 2000 cm⁻¹ in the ir spectra. The 2000-cm⁻¹ peak is always accompanied by a smaller one (often in the form of a weak shoulder) at ~2100 cm⁻¹. The general assignment of this second peak is to SiH₂ groups,^{1,2} but singly bonded H at microvoid surfaces is also invoked^{3,4} and even the combination of both at a time has been suggested.⁵ In our study we refer to the 2100-cm⁻¹ peak as a SiH₂ vibration, but this choice does not restrict in any way the physical considerations and conclusions made.

A subject of special interest is the study of ultrathin (~10–100 Å) plasma-deposited *a*-Si:H films because of their use in large-surface electronics. A number of workers in the field have carried out sensitive *in situ* ir measurements in order to get better insight into the growth mechanisms of *a*-Si:H thin films and the role of H played in them.^{6–9} It is important to note that in ultrathin *a*-Si:H layers boundary effects become non-negligible and can modify the vibrational properties of the material. Thus Toyoshima *et al.*,⁹ in their studies on the growing *a*-Si:H surface using ir reflec-

tance spectroscopy, noticed a weak feature below 2000 cm⁻¹ that was attributed to the existence of a subsurface H-rich region. Moreover, their spectra reveal a thickness-dependent position of this low-frequency vibration, which, however, was not studied. It is interesting to note that Katiyar *et al.*⁸ detected the same low-frequency feature under similar experimental conditions, but obviously did not notice its presence in their spectra. Studying the Si-H bond in ultrathin *a*-Si:H films by ir ellipsometry, Blayo, Blom, and Drévilion¹⁰ evidenced the thickness dependence of the SiH stretching frequency and assumed it was due to morphological changes of the material in the vicinity of the interface.

In this work we systematically study the thickness-dependent shift in the vibrational frequency of the Si-H stretching mode in SiH and SiH₂ bonding configurations in *a*-Si:H. Because of its high sensitivity and possibility of performing *in situ* measurements, infrared phase-modulated ellipsometry is particularly well adapted to the study of thin-film materials¹¹ and is the basic technique used in the present work. In order to explain and model the experimental results we consider several physical effects and finally relate the frequency shift phenomenon to a change in the structural properties of the *a*-Si:H network. Together with discussing the physical origins of such structural changes, we propose a corresponding analytical model that helps to quantify the qualitative physical picture suggested.

II. EXPERIMENTAL DETAILS

Undoped *a*-Si:H samples were deposited *in situ* by a rf glow discharge (13.56 MHz) decomposition of pure silane (SiH₄) under the following common device-quality conditions:¹² rf power of 50 mW/cm², 70-mTorr silane pressure, and a flow rate of 12 SCCM (where SCCM denotes cubic centimeter per minute at STP). Residual pressure in the chamber before deposition was typically of the order of 10⁻⁵

mbar. Gases used in doping were diborane (B_2H_6 , *p* doping), trimethylboron [$(CH_3)_3B$, *p* doping], and phosphine (PH_3 , *n* doping). In both sorts of doping a gas-flow ratio of 2:12 SCCM (with respect to silane) was fixed, the total pressure in the reactor being maintained constant. All doping gases were 98% hydrogen diluted. Three substrate temperatures were studied: 110 °C, 180 °C, and 250 °C. The default value was 180 °C unless otherwise stated. Corning 7059 glass, fused silica, crystalline Si(100), and chromium (1000 Å of Cr evaporated on Corning glass) were used as substrates. All substrates were chemically cleaned, but no special treatment for removing passivating surface overlayers was performed. Growth rates were estimated to be ~ 1.1 Å/s (undoped and *n*-doped *a*-Si:H) and ~ 1.4 Å/s (*p*-doped *a*-Si:H) using UV-visible spectroscopic ellipsometry (UVISEL from ISA Jobin-Yvon) on thick (~ 5000 Å) samples. Film thicknesses ranged from 100 to 4000 Å. The thickness values are direct conversions of the deposition times using the above growth rates.

The vibrational properties of the *a*-Si:H films were measured *in situ* using a sensitive infrared phase-modulated ellipsometer described in detail elsewhere.¹³ The instrument is coupled to the reactor, thus enabling the *in situ* characterization of the growing films. The incidence angle is fixed at 70°. Measurements of the ellipsometric parameters ψ and Δ were recorded *in situ* between two consecutive depositions in the spectral range from 1900 to 2200 cm^{-1} with a resolution estimated to be 5 cm^{-1} . The samples were kept at the deposition temperature during the spectra recording. Precision on the ellipsometric angles is 0.01° on ψ and 0.005° on Δ . A nitrogen-cooled InSb detector was used. Typically, a spectrum was recorded in 12 min.

III. RESULTS

Before discussing the experimental ellipsometric spectra, a brief presentation of the parametrization used in our measurements is necessary. The usual ellipsometric parameters $\rho = \tan\psi \exp(i\Delta)$ are represented in the form of the complex optical density¹⁴ $D = \ln(\bar{\rho}/\rho)$, where $\bar{\rho}$ refers to the substrate before film deposition. Such a parametrization is used because, in the special case of thin films, ReD (ImD) is directly proportional to the imaginary (real) part of the film dielectric function ϵ (Re and Im stand for real and imaginary parts, respectively). The contribution of a vibration mode to the

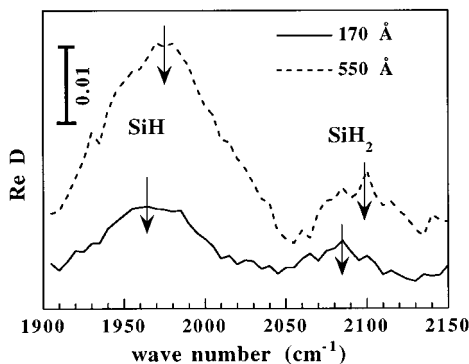


FIG. 1. Real part of the optical density for two *a*-Si:H films deposited on glass at 180 °C with different thicknesses: 170 and 550 Å.

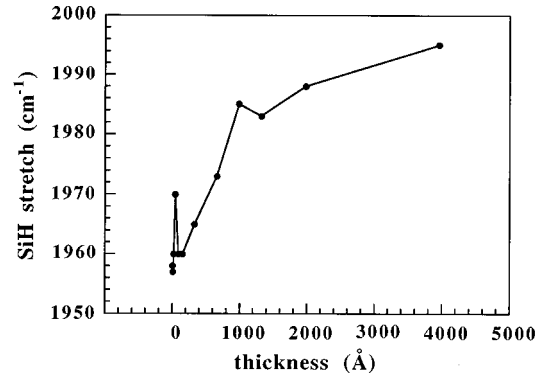


FIG. 2. SiH-group vibrational frequency as a function of the film thickness for *a*-Si:H deposited on glass at 180 °C.

film dielectric function can be estimated from the Lorentz harmonic-oscillator expression

$$\epsilon = \epsilon_{\infty} + \frac{F}{\omega_0^2 - \omega^2 - i\Gamma\omega}, \quad (1)$$

where ω_0 is the vibrational frequency, Γ is a phenomenological damping parameter, and F is the oscillator strength, related to the high- and low-frequency dielectric constants of the material ϵ_0 and ϵ_{∞} , respectively, by the expression $F = \omega_0^2(\epsilon_0 - \epsilon_{\infty})$. Thus the presence of a vibration mode of a chemical bond at a frequency ω_0 is revealed by an extremum in ReD spectrum that can be a maximum or a minimum depending on the substrate dielectric function. For all substrates used in this study, except for the *c*-Si one, the ReD spectrum exhibits a maximum value for a given chemical bond vibration.

The ellipsometric spectra in the Si-H stretching region of two *a*-Si:H films with different thicknesses, 170 and 550 Å, are presented in Fig. 1. Both films are deposited on Corning glass substrates. The SiH- and SiH₂-group stretching vibrations are clearly identified by the respective peaks in the ReD spectra. Both SiH and SiH₂ vibrations have lower frequencies compared to the reported bulk values (2000 and 2100 cm^{-1} , respectively¹). Furthermore, a shift towards lower frequencies is observed for both vibrations with decreasing film thickness.

The SiH and SiH₂ peak positions as functions of the film thickness are shown in Figs. 2 and 3, respectively. The vi-

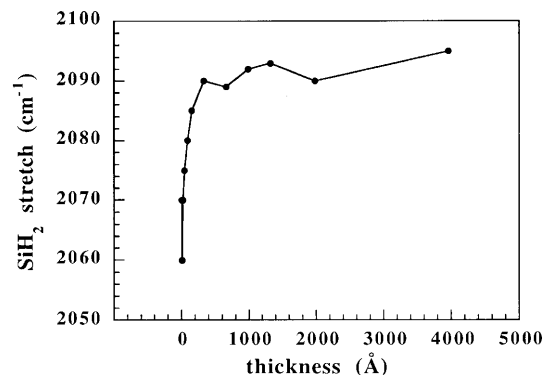


FIG. 3. SiH₂-group vibrational frequency as a function of the film thickness for *a*-Si:H deposited on glass at 180 °C.

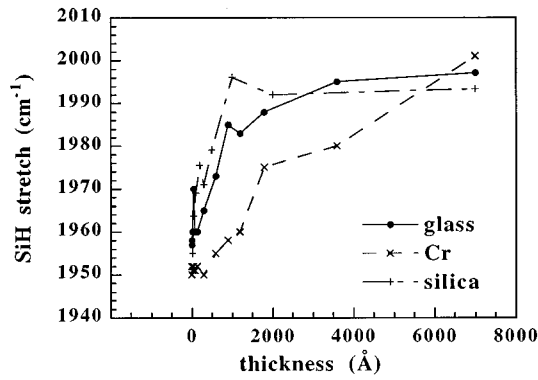


FIG. 4. SiH-group vibrational frequency as a function of the film thickness for *a*-Si:H deposited on three different substrates: glass, fused silica, and Cr at 180 °C.

brational frequencies were determined by fitting of the peaks to a Lorentzian [see Eq. (1)] with an error of $\sim 5 \text{ cm}^{-1}$ at small thicknesses where the signal-to-noise ratio was too small. Both vibrational frequencies increase with thickness and asymptotically tend to their bulk values (2000 and 2100 cm^{-1}). Notice that the bulk frequency is achieved more rapidly in the SiH_2 -vibration case.

Figure 4 shows the thickness dependence of the SiH stretching mode frequency for *a*-Si:H films deposited on three different substrates: Corning glass, fused silica, and Cr. The qualitative behavior of all the curves is similar: a start from a low initial frequency followed by an asymptotic trend to the bulk value with growing thickness. The rate of change of the vibrational frequency with film thickness is, however, substrate dependent. It is interesting to note that the initial frequencies (i.e., the frequencies at infinitely small thicknesses) are almost identical (to the accuracy of the vibrational frequency determination) for all the substrates used in this study.

The deposition-temperature dependence of the frequency shift is illustrated in Fig. 5, where the SiH group frequency versus thickness is plotted for *a*-Si:H films deposited on glass substrates at three temperatures: 110 °C, 180 °C, and 250 °C. A clear trend is evidenced, namely, the higher the deposition temperature, the steeper the approach to the bulk frequency.

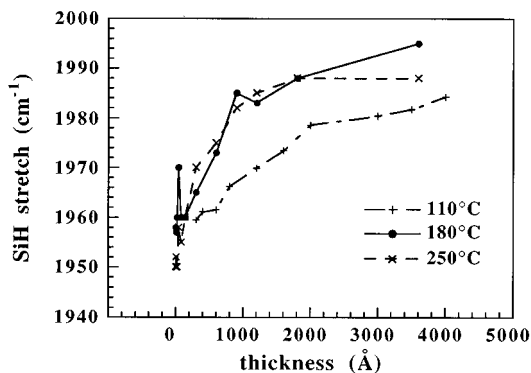


FIG. 5. SiH-group vibrational frequency as a function of the film thickness for *a*-Si:H deposited on glass at three different temperatures: 110 °C, 180 °C, and 250 °C.

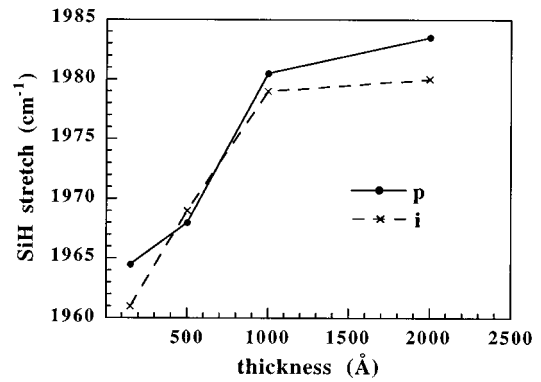


FIG. 6. SiH-group vibrational frequency as a function of the film thickness for intrinsic and *p*-doped *a*-Si:H deposited on glass at 180 °C.

Doping is known to modify the concentrations of SiH_n ($n=1, 2,$ and 3) groups in *a*-Si:H,¹⁵ hence its possible influence on the vibrational properties of the material cannot be *a priori* excluded. However, doping seems to have no detectable effect on the frequency shift phenomenon, as can be seen from Fig. 6, where the frequency-versus-thickness curves of intrinsic and *p*-doped *a*-Si:H films on glass are presented. Similar results are obtained for *n*-doped films. Obviously, the observed shift effect is not influenced by the presence of doping (or, more generally, impurity) atoms in the *a*-Si:H matrix.

IV. DISCUSSION

In order to understand the physical phenomenon lying in the origin of the experimentally observed thickness-dependent Si-H vibrational frequency shifts we shall discuss in some detail the possible effects leading to frequency changes.

A. Possible physical interpretations of the frequency shift

1. Optical effect

It is well known from ir transmission and reflection spectroscopy studies of thin-film materials on different substrates that the positions of the vibrational frequencies of the material can be thickness dependent. This is the case, for example, of amorphous silicon oxide (*a*- SiO_x) (Ref. 16) and amorphous silicon nitride (*a*- SiN_x) (Ref. 17) on *c*-Si substrates. It has been shown by simulations that the thickness-dependent line shift is due to Fresnel reflections at the interfaces in the film-on-substrate optical system¹⁸ and is a pure second-order optical effect inherent to the specific thin-film configuration.¹⁹ The magnitude of the shift is directly dependent on the absorption line strength. In the limit of infinitely thin film the observed vibrational frequency corresponds to the bulk line strength and gradually departs from its value with growing film thickness.

In Fig. 7 a simulation of $\text{Re}D$ in the region of Si-H stretching vibration as a function of the *a*-Si:H film thickness is shown. A harmonic oscillator with the parameters $\epsilon_\infty=9$, $\omega_0=2000 \text{ cm}^{-1}$, $F=4 \times 10^4 \text{ cm}^{-2}$, and $\Gamma=80 \text{ cm}^{-1}$ was used. These parameters were obtained by fitting literature data on

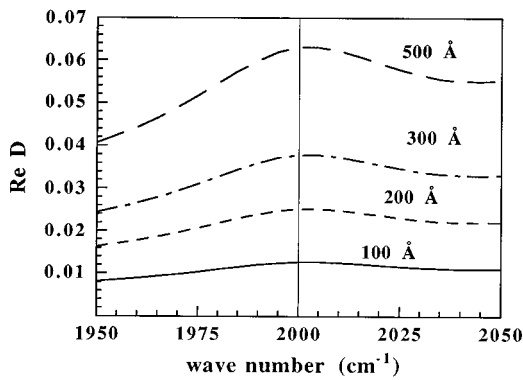


FIG. 7. Simulation of $\text{Re } D$ of $a\text{-Si:H}$ films with different thicknesses on a glass substrate in the SiH stretch region.

$a\text{-Si:H}$ dielectric function²⁰ to the Lorentzian expression (1). An experimentally measured Corning glass sample was used as a substrate. The results clearly reveal a thickness-independent vibrational frequency, systematically upshifted by about 3 cm^{-1} from its "standard" value (2000 cm^{-1}). Therefore, the above optical effect on thin-film vibrational frequencies cannot account for our experimentally observed shifts, in spite of its general nature. It is also important to note the substantial difference between the optically induced shift and the one observed in our measurements, namely, the observed frequency departs from its bulk value with growing film thickness in the former, while it tends to its bulk value in the latter.

2. Presence of contaminants

The common feature of some of the substrates used in this study (namely, $c\text{-Si}$ and Cr ones) is the presence of a surface oxide overlayer, since no special surface treatment was performed prior to the $a\text{-Si:H}$ deposition. (Note that there is no such oxide overlayer on the deposited $a\text{-Si:H}$ film surface since all measurements in this study are done *in situ*.) It is well established that Cr and Si are covered by $\sim(20\text{--}30)\text{-\AA}$ -thick passivating oxide layers,²¹ which are thermally stable in the temperature range studied here. Furthermore, the methyl (CH_3) and hydroxyl (OH) groups are known to be common contaminants of air-exposed metal surfaces.²² On the other hand, the glass substrate is known to influence the vibrational properties of the interface layer during film deposition through a chemical interaction.²³ Therefore, in all cases studied, it is quite possible for an interaction between substrate overlayers (or substrates themselves) containing native oxides and/or methyl (hydroxyl, amine) groups and the growing film to take place. In such manner, a shift in the SiH (SiH_2) vibrational frequencies may occur as a result of the difference in the local chemical environment with respect to the bulk in the intermixing layer formed at the film-substrate interface. This phenomenon, known as the chemical induction effect, was studied and quantitatively described by Lucovsky.²⁴ In his model, a linear relationship between the SiH (SiH_2) stretching frequencies and the electronegativity of the first neighbors to the SiH (SiH_2) groups was established. Experimental studies of amorphous-silicon oxides obtained by silane oxidation have given the value of $\sim 2100 \text{ cm}^{-1}$ of the Si-H stretching vibration frequency,²⁵ in full

agreement with the predicted one (2103 cm^{-1}). More generally, since all possible contaminants susceptible of changing the local environment of the Si-H stretching vibration have atomic electronegativities^{24,26} (O, 5.21; C, 3.79; H, 3.55; and N, 4.49) higher than that of the substituted Si atom(s) (Si, 2.62), the chemical induction shift, if observed, is always positive. Furthermore, secondary-ion-mass spectroscopy measurements carried out for $a\text{-Si:H}$ samples deposited under very similar conditions to ours showed a negligible oxygen content ($\leq 10^{19} \text{ cm}^{-3}$) in $a\text{-Si:H}$ at the interface, independently of the substrate used.²⁷ Using the above content, one can estimate the upper limit of the chemically induced upshift to be about 4 cm^{-1} . Therefore, the hypothesis of the presence of substrate contaminants being the cause of the experimentally observed low-frequency shift should be ruled out.

An interesting modification of the above idea is interpreting hydrogen in $a\text{-Si:H}$ as a "contaminant" changing the local environment of the Si-H bond. It is a well-established fact that in plasma-deposited $a\text{-Si:H}$ there is a hydrogen accumulation at a few-monolayers level at the film-substrate interface, as well as at the film surface.^{6,7} This high-H concentration results in morphological changes of the Si matrix, a decrease of the dielectric constant of the material, and a chemically induced frequency shift of the type already discussed. Using the chemical induction model, Tsu and Lucovsky²⁸ have shown that the Si-H stretching vibration shifts to higher frequencies with hydrogen concentration in plasma-deposited $a\text{-Si:H}$ films and therefore the chemically induced shift due to the hydrogen excess at the film boundaries has once more an opposite direction compared with our experimental results.

3. Interface-surface defect states

The presence of residual unpaired spins (singly occupied dangling bonds) in device-quality $a\text{-Si:H}$ (Ref. 29) was recognized earlier by electron-spin resonance measurements. Later, the thickness dependence of the defect concentration was evidenced using photothermal deflection spectroscopy.^{30,31}

It is straightforward to show, using the previously discussed chemical induction model, that the presence of a dangling-bond defect as a nearest neighbor of a SiH group will result in a decrease of the Si-H bond stretching frequency. Thus attributing zero electronegativity to the dangling bond (further denoted by d) and using the semi-empirical formula given by Lucovsky,²⁴ one obtains the value of $\sim 1930 \text{ cm}^{-1}$ for the vibrational frequency of the $\text{SiH}(d\text{Si}_2)$ structure. Thus some spectral lines in the $1840\text{--}1960 \text{ cm}^{-1}$ range observed in H-implanted $c\text{-Si}$ using ir-absorption spectroscopy were tentatively assigned to dangling-bond defects,²⁶ in the frame of the chemical induction effect. Following this model, the thickness-dependent vibrational frequency may be regarded as an average value resulting from the superposition of two absorption peaks, one at about 1930 cm^{-1} , corresponding to defects situated in a thin layer at the film surface or interface, and another one at 2000 cm^{-1} , standing for the "normal" Si-H bond stretching frequency in the bulk $a\text{-Si:H}$. Under the assumption of independence of the Si-H oscillator strength on the presence of defects, one obtains ~ 0.1 for the ratio of dangling bonds to

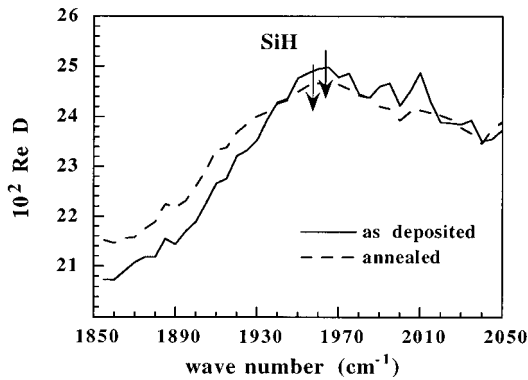


FIG. 8. Real part of the optical density in the SiH stretching region for a 550-Å-thick *a*-Si:H film deposited on glass at 110 °C before and after 4 h of annealing at 250 °C.

silicon atoms. The value of $5 \times 10^{22} \text{ cm}^{-3}$ for the concentration of Si atoms in *a*-Si:H (Ref. 32) leads to some $5 \times 10^{21} \text{ cm}^{-3}$ defects in the surface-interface layer. The last value is by four orders of magnitude higher than the experimentally determined surface defect density ($3 \times 10^{17} \text{ cm}^{-3}$) in plasma-deposited *a*-Si:H.³¹ It is interesting to note that, as shown by Oguz *et al.*³³ in their studies on ion-bombardment created defects in *c*-Si, reversible changes in the Si-H oscillator strengths may take place. However, the changes reported by Oguz *et al.* can account for not more than an order of magnitude in the above difference between experimental and calculated defect concentrations.

Further unfavorable evidence for the dangling-bond model is the relatively constant initial frequency (see Figs. 4 and 5) independent of the substrate nature and temperature. However, according to the dangling-bond model, the higher the substrate temperature, the higher the initial frequency, while in our case all curves start from the value $\sim 1950 \text{ cm}^{-1}$ in the limit of very thin films.

The possibility of a practical verification of the dangling-bond model is suggested by the defect annealing effect. The reduction of defects under annealing (by up to an order of magnitude³¹) due to the enhanced hydrogen diffusion in the as-deposited material is a well-known behavior of *a*-Si:H. In the frame of the defect model such an annealing-produced defect reduction would lead to an opposite shift of the Si-H vibrational frequency back to its “normal” bulk value (2000 cm^{-1}). Following the above idea, *in situ* annealing of a plasma-deposited *a*-Si:H film was performed. A 550-Å-thick film deposited at 110 °C was annealed for 4 h at 250 °C. Vibrational spectra in the SiH bond stretching region were measured before and after annealing. The results are shown in Fig. 8. A very small shift to lower frequencies, instead of an upshift towards the bulk frequency, is observed. Therefore, the dangling-bond defect model cannot account for the experimentally observed low-frequency shift.

4. Phonon coupling

It is interesting to note that fitting the SiH peak before and after annealing to a Lorentzian expression in order to estimate more accurately the vibrational frequencies gives, for the temperature slope of the small downshift, $0.036 \text{ cm}^{-1}/\text{K}$ (see Fig. 8). This value is in excellent agreement with the

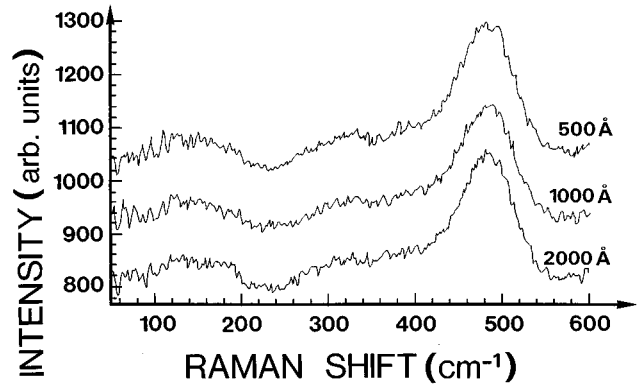


FIG. 9. Raman scattering spectra of three *a*-Si:H films deposited on glass at 250 °C with different thicknesses: 500, 1000, and 2000 Å.

one ($0.035 \text{ cm}^{-1}/\text{K}$) determined by Grimal *et al.*³⁴ in their recent studies on the weak phonon coupling to the Si-H stretching modes in *a*-Si:H. They showed that the coupling between an *a*-Si:H-lattice phonon and the Si-H stretching mode resulted in a temperature-dependent reversible shift of the vibrational frequency of the latter. In order to evidence any thickness dependence of an *a*-Si:H phonon mode susceptible of coupling to the Si-H stretching frequencies and thereby, of shifting them, we performed *ex situ* Raman scattering measurements on three *a*-Si:H films deposited at 250 °C on Corning glass with three different thicknesses: 500, 1000, and 2000 Å. Argon-laser excitation at 514.5 nm was used. The spectra measured in the lattice phonon range from 50 to 600 cm^{-1} are shown in Fig. 9. All phonon modes [TA, 150 cm^{-1} ; LA, 310 cm^{-1} ; LO, 380 cm^{-1} , and TO, 480 cm^{-1} (Ref. 35)] identified as peaks or shoulders in the spectra apparently exhibit no thickness-dependent intensities, at least in the thickness range studied. Furthermore, as already noted, experimental frequency shifts due to coupling with the above lattice phonon have opposite signs to our thickness-dependent shift. It is clearly unrealistic to imagine the $\sim 50\text{-cm}^{-1}$ shift from the Si-H stretching bulk frequency as due to a thickness-dependent phonon coupling to an ir vibration mode.

5. Intrinsic stress

It is a well-established experimental fact that stress in the material can influence the vibrational frequencies of the different chemical bonds present through the introduction of bond strain. Thus, in proton-implanted crystalline silicon the Si-H stretching line presumably due to a H-saturated monovacancy-type defect in the *c*-Si matrix shifts from 2062 to 2070 cm^{-1} with the application of a uniaxial mechanical stress of 600 MPa.³⁶ The explanation of this effect lies in the modification of the force constants with the change of bond lengths under the applied mechanical constraints. However, such bond strain can result not only from external mechanical forces, but also from the intrinsic stress inherent to the material or its special geometry. In their studies on H-saturated Si(100) surface, Chabal and Raghavachari³⁷ showed, using high-resolution ir reflectance spectroscopy, that the Si-H stretching frequency is upshifted by $\sim 7 \text{ cm}^{-1}$

because of the decrease in the Si-H atomic distances at the crystal surface.

The intrinsic stress in amorphous materials, in the same manner as in crystalline materials, may cause shifts in the vibrational frequencies. However, these stress-induced shifts cannot be theoretically estimated and, consequently, are being experimentally determined. Thus it has been shown for plasma-deposited silicon nitride ($a\text{-SiN}_x\text{:H}$) films that the frequency of the Si-H stretch increases by $\sim 10\text{ cm}^{-1}$ with an increase in compressive film stress up to 300 MPa.³⁸ On the other hand, Si-H stretching frequency in plasma-deposited silicon carbide ($a\text{-SiC:H}$) films exhibited no stress dependence in the large range from -1000 MPa (compressive) to $+800$ MPa (tensile) stress.³⁹

Plasma-deposited $a\text{-Si:H}$ films are known to grow under high compressive stress.⁴⁰ Values as high as 1200 MPa for doped films have been reported.⁴¹ The stress in $a\text{-Si:H}$ is a consequence of the overcoordinated amorphous Si network,⁴² which does not relax significantly after growth, as well as of the presence of hydrogen.^{43,44} However, to the authors' knowledge, there is no reported evidence on stress-induced vibrational frequency shifts in $a\text{-Si:H}$. Several workers have shown that the compressive stress in plasma-deposited $a\text{-Si:H}$ films is dependent on the substrate nature and temperature.^{45,46} Using the published data,⁴⁵ it is easy to determine that the stress grows from 100 MPa at 110°C to 500 MPa at 250°C , i.e., five times. However, the same argument as for the dangling-bond model holds in this case too, namely, the initial frequencies in our experimental curves are temperature and substrate independent.

Similarly, low-temperature (300°C) annealing of plasma-deposited $a\text{-Si:H}$ films was shown to reduce the compressive film stress more than three times (from 640 to 200 MPa).⁴³ In our annealing experiment, however, the $a\text{-Si:H}$ film exhibited no stress-induced frequency shift (see Fig. 8 and the related discussion).

The above considerations lead to the conclusion that the intrinsic film stress have no direct effect on the Si-H stretching frequency in $a\text{-Si:H}$. Nevertheless, as we shall see, the strained amorphous-Si network can influence indirectly the Si-H vibrational frequency.

6. Variation of the dielectric constant

The vibrational properties of $a\text{-Si:H}$ can be adequately described in terms of the so-called polarized medium model.^{1,47-49} In this model the material is considered to consist of Si-H bonds uniformly embedded in a homogeneous $a\text{-Si}$ matrix. The Si-H dipole, supposed to reside in a microscopic cavity, polarizes the surrounding medium, which, in its turn, reacts on it by its depolarization (or reaction) field. This represents the well-known Onsager local field model, initially applied to calculating the polarizabilities of polar liquid solutions.⁵⁰ Later, the reaction field has the effect of lowering the vibrational frequency of the immersed dipole. This phenomenon, usually called the solid-state effect, allows one to obtain the vibrational frequency of a dipole embedded in a solid, knowing the frequency of the free dipole. It was applied with success by Cardona⁴⁹ to the calculation of the Si-H stretch frequencies in $a\text{-Si:H}$ using their values in gaseous silanes. The frequency shift is given by the formula (in cgs units)

$$\Delta\omega = -\frac{e^{*2}}{\mu\omega_0 R^3} \frac{\varepsilon - 1}{2\varepsilon + 1}, \quad (2)$$

where R is the radius of the cavity containing the dipole, e^* is the effective dynamical charge of the dipole, ω_0 and μ are its vibrational frequency (in s^{-1}) and reduced mass, respectively, and ε is the ir dielectric constant of the host matrix, assumed to be nonabsorbing (i.e., $\text{Im } \varepsilon = 0$). This relationship, known as the Kirkwood-Bauer-Magat formula, is widely used in ir spectroscopy of liquid solutions.⁵¹ We shall discuss in some detail each of the quantities entering the above expression, since this will be of importance in the following.

The effective dynamical charge e^* arises from changes in charge distributions as the atoms vibrate and should not be confused with the static charge, which is a result of the different electronegativities of the atoms in the dipole. The dynamical charge is the one participating in the ir activity of $a\text{-Si:H}$ and its value depends on the Si-H bond configuration (SiH, SiH₂, or SiH₃ group), as well as on the vibrational mode (stretching, bending, wagging, etc.).

The vibrational frequency of the free Si-H dipole in the case of the SiH group is in fact the stretching frequency of the virtual structure SiH(Si₃). Using a valence force field model, Cardona calculated the value 2099 cm^{-1} for the Si-H stretch of SiH(Si₃). By *ab initio* Bethe lattice calculations Jing, Whitten, and Lucovsky⁵² obtained 2132 cm^{-1} . We used the value 2100 cm^{-1} in our study. For the SiH₂ group, the value 2128 cm^{-1} as given by Cardona's valence force field model was taken. It is noteworthy that all the frequencies reported differ by less than 4% and their exact values are not of decisive importance to the accuracy of the model used. Following Cardona,⁴⁹ the reduced mass μ was taken to be equal to the H atomic mass, while for the ir dielectric constant ε of the host medium the $c\text{-Si}$ value of 12 was used.

Maybe the less-well-defined quantity entering Eq. (2) is the cavity radius R . Although the existence of small atomic vacancies with strong electrostatic screening containing H atoms has been theoretically⁵³ and experimentally (by small-angle x-ray-scattering measurements⁵⁴) suggested, no experimental attempts to estimate the cavity dimensions have been made so far, mainly because of the insufficient instrumental resolution on the scale of angstroms. Cardona obtained excellent agreement with experiment by setting R equal to the covalent radius of the Si atom ($r_{\text{Si}} = 1.17\text{ \AA}$). By definition, r_{Si} equals one-half of the Si-Si bond length in $c\text{-Si}$ or one-half of the average Si-Si bond length in $a\text{-Si:H}$ too.³³ Extensive experimental studies on vibrational frequency shifts of molecules in liquid solutions showed that R is related to the molecular volume of the solvent rather than to the solute volume whether the solvent molecules are larger or smaller than the solute molecules.^{55,56} In this way, R appears to be a characteristic parameter of the embedding matrix rather than of the immersed dipole. This experimental evidence may constitute a justification for using the value of 1.17 \AA in our model calculations.

Let us suppose now that for some physical reason the dielectric constant of the $a\text{-Si}$ matrix lowers its value at the film interface or surface. For example, it is well known that the increase of H concentration at the growing film surface or interface results in a lower refractive index of the material.⁵⁷

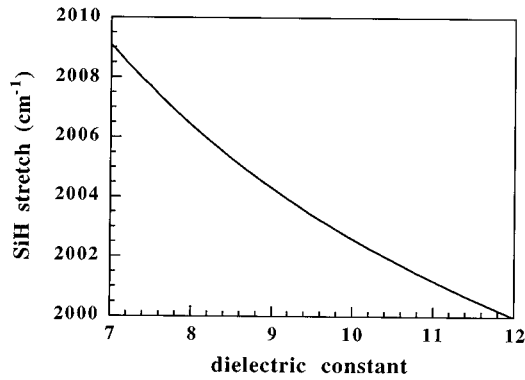


FIG. 10. SiH stretch vibrational frequency as a function of the dielectric constant of the medium.

It is also possible that under certain deposition conditions, incomplete island coalescence, particulates incorporation, or some other inhomogeneities at the film-substrate interface during the growth take place, resulting in microvoids formation⁵⁸ and thereby lowering the material dielectric constant. Thus the imperfect coalescence during the initial columnar growth of plasma-deposited *a*-Si:H films on different (metal and *c*-Si) substrates have been evidenced by uv-visible kinetic ellipsometry.^{59–62} In the special case of *a*-Si:H growth on a glass substrate nucleation does not take place, yet a film-substrate interaction leading to a lower interface refractive index has been clearly revealed using ir (Ref. 10) and uv-visible⁶¹ ellipsometry techniques.

The effect of the decrease of the dielectric constant on the Si-H vibrational frequencies can be easily modeled by using Eq. (2) and by taking the above values for the parameters in it. Thus, varying ϵ from 12 down to 7 in Eq. (2) results in the curve in Fig. 10. It is clearly seen that the SiH group vibrational frequency increases by about 9 cm^{-1} with decreasing ϵ . However, this behavior is opposite the experimentally observed one in our spectra. Therefore, the assumption of a decreased dielectric constant of the material at its surface or interface should be discarded.

B. Interface structural disorder

The structural disorder in *a*-Si:H has been the subject of a great number of studies. It is well established now that bond length and especially bond-angle distortions are responsible for the Raman and ir activity of *a*-Si.⁶³ Moreover, hydrogen incorporation in *a*-Si:H was shown to reduce the bond-length fluctuations⁶⁴ and, consequently, is susceptible of modulating the degree of network disorder by its spatial distribution.⁶⁵ Therefore, Raman scattering measurements on *a*-Si:H are supposed to reflect any change in the structural order of the material. For example, TO Raman peak position and width are shown to depend on bond-angle distortions in the *a*-Si:H network.^{66,67} Thus a thickness-dependent increased disorder in the *a*-Si:H interface in *a*-Si:H/*a*-SiN_x superlattices has been evidenced.⁶⁸ A similar behavior of the interface disorder in *a*-Si:H deposited on different substrates (glass, silicon, and steel) was detected by Hishikawa *et al.*,²⁷ who evidenced the existence of an $\sim 0.1\text{-}\mu\text{m}$ -thick interface layer with structural properties different from the bulk ones.

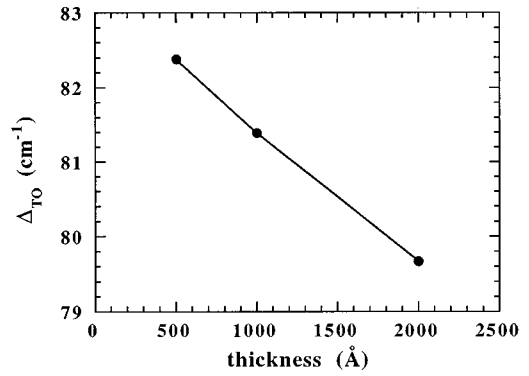


FIG. 11. Thickness dependence of the TO-like peak width for *a*-Si:H films deposited on glass at 250 °C.

In order to characterize the structural disorder in our samples we performed *ex situ* Raman scattering measurements on *a*-Si:H films obtained under different deposition conditions. Figure 11 shows the TO-like peak width Δ_{TO} for *a*-Si:H films deposited at 250 °C on Corning glass substrates as a function of the film thickness. The measurements were performed using a 514.5-nm Ar laser excitation. As noted, Δ_{TO} is a direct measure of short-range structural order, being approximately proportional to the bond-angle distribution width $\Delta\theta$.⁶⁷ The curve clearly reveals an increasing disorder with decreasing the film thickness. This behavior indicates that bond-angle distortions are most significant at the film interface or surface.

A similar trend is evidenced in Fig. 12, where the disorder profiles of two series of films deposited at 180 °C on Corning glass and Cr substrates are compared. A 632.8-nm HeNe laser excitation was used. It is easily seen in the figure that the bond-angle fluctuations are more important in the *a*-Si:H film deposited on Cr substrate in comparison to the glass substrate. Moreover, a careful inspection of Figs. 11 and 12 shows that disorder is larger in the 500-Å-thick *a*-Si:H on glass deposited at 180 °C compared to the 250 °C one, having in mind the penetration depths of both laser lights used: 700 Å for Ar (green) and 5000 Å for HeNe (red).

The thickness dependence of disorder in *a*-Si:H films revealed by Raman scattering measurements readily compares with the thickness-dependent vibrational frequency shift in ir ellipsometry measurements on these films. Moreover, both

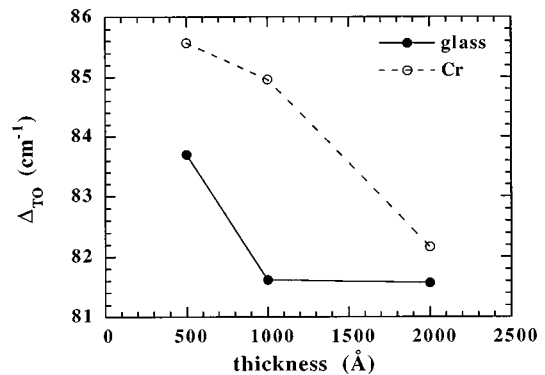


FIG. 12. Thickness dependence of the TO-like peak width for *a*-Si:H films deposited on glass and Cr at 180 °C.

TABLE I. Possible physical causes of a vibrational frequency shift in *a*-Si:H with their approximate magnitudes and shift directions. [The symbol (?) stands for a theoretical estimate.]

Frequency shift cause	Approximate magnitude (cm ⁻¹)	Shift direction (to higher or lower frequencies)
optical effect	3	higher
substrate contamination	4	higher
interface-surface defect states	0.05(?)	lower
phonon coupling	5	higher
intrinsic stress	10(?)	higher or lower
variation of the dielectric constant	5	higher
structural disorder	30	lower

disorder and vibrational frequency profiles exhibit a similar temperature and substrate dependence. Furthermore, Raman spectroscopy measurements have revealed that the structural randomness of the *a*-Si network in the initial stages of the film deposition is independent on the deposition conditions.⁶⁸ A similar case is that of our ir ellipsometry measurements in which the initial vibrational frequencies do not depend on the substrate nature or temperature, nor on film doping. Consequently, according to the Raman measurements, the initial vibrational frequencies in our spectra (~ 1950 and ~ 2050 cm⁻¹) are to be attributed to the most disordered *a*-Si:H at the interface.

These observations suggest that a correlation between the ir frequency shift and the structural disorder in *a*-Si:H thin films may be established. It is important to note that there have been several experimental studies relating the ir vibrational properties of Si to disorder. Thus Stein and Peercy⁶⁹ observed the Si-H stretch mode at 1985 cm⁻¹ in highly disordered H-implanted *c*-Si. Chabal, Higashi, and Christman,⁷⁰ in their studies of hydrogen chemisorption on Si(111), attributed an unidentified mode at 1970 cm⁻¹ to Si-H bonds arising from H diffusion and random bonding in the subsurface layer. In another study on the same subject, Chabal⁷¹ attributed the downshift of the Si-H surface vibration mode at 2073 cm⁻¹ to its screening by the silicon environment. Moreover, these studies suggest that dielectric screening adequately models the influence of the structural disorder in the material on its vibrational properties. A concise review of the previously discussed possible physical causes for the vibrational frequency shifts, together with their approximate magnitudes and shift directions, is presented in Table I.

1. Modeling of the frequency shifts

Here we shall argue that the structural disorder in the *a*-Si network at the film-substrate interface can indirectly influence the ir vibrational properties of the material and, in particular, is mostly (if not entirely) responsible for the thickness-dependent downshift of the Si-H stretching mode frequency. In order to show this, we need to discuss a slight generalization of the polarized medium model already presented. Instead of considering a spherical cavity containing the Si-H dipole, one may take a cavity of some other form, say, an ellipsoidal one. A new parameter describing the depolarization effect, the geometrical factor *A* varying within 0 and 1, is introduced. In the extreme cases of a rod and a slab *A* equals 0 and 1, respectively; for a sphere $A = \frac{1}{3}$. In the frame of the ellipsoid model,⁷² Eq. (2) takes the form

$$\Delta\omega = -\frac{e^{*2}}{\mu\omega_0} \frac{3}{2abc} \frac{A(1-A)(\varepsilon-1)}{\varepsilon+(1-\varepsilon)A}, \quad (3)$$

where *a* and *b* = *c* are the semiaxes of the rotational ellipsoid cavity. If one assumes a small departure from the spherical form, Eq. (3) may be reduced to

$$\Delta\omega = -\frac{e^{*2}}{3\mu\omega_0 R^3} \frac{\varepsilon-1}{\varepsilon+(1-\varepsilon)A}, \quad (4)$$

where an ‘‘effective’’ cavity radius *R* defined by the mean-geometric relationship $R^3 = abc$ has been introduced.

From a microscopic viewpoint, the introduction of a form different from the spherical one for the cavity in the polarized medium model reflects the structural disorder present in the *a*-Si network at the interface under the form of bond-angle (or -length) distortion. Since the Si-H bonds are isotropically distributed in the Si matrix, the factor *A* in (4) is an effective quantity obtained by spatially averaging the factors *A_e* of a distribution of randomly oriented ellipsoids. By averaging the polarizabilities of the ellipsoids,⁷² the expression for *A* can be obtained

$$A = \frac{2\varepsilon - 3(\varepsilon - 1)A_e(1 - A_e)}{5\varepsilon + 1 - 3(\varepsilon - 1)A_e}. \quad (5)$$

Thus, having determined experimentally the value of *A* one can, in principle, obtain the departure from the spherical form expressed by the difference between *A_e* and $\frac{1}{3}$.⁷³ One should not forget, however, that the polarized medium model is an idealized one and hence any direct physical interpretations should be made with caution. It is expected to describe adequately the vibrational properties of the disordered material but not its microstructure, although based on a straightforward physical picture.

It is relatively easy to see that with the factor *A* increasing from $\frac{1}{3}$ up to 1 the absolute value of the frequency shift $\Delta\omega$ given by Eq. (4) increases. Moreover, it can be shown that the factor *A* calculated with the help of (5) is always larger than $\frac{1}{3}$ whatever the values of *A_e* ($0 < A_e < 1$) and ε (for a real ε). Therefore, our model always predicts a downshift of the vibrational frequency in the case of a distorted network.

In order to model our experimental data we have to analytically describe the dependence of the disorder on the film thickness. If we assume that the amplitude of the *a*-Si matrix distortions decays exponentially from the interface, the factor *A* at a distance *z* can be written as

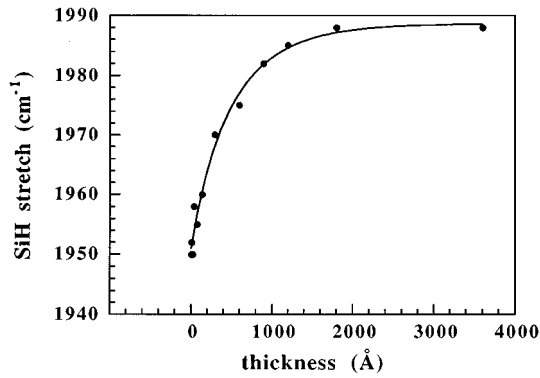


FIG. 13. Fit of the SiH-group vibrational frequency as a function of the film thickness for *a*-Si:H deposited on glass at 250 °C.

$$A = \Delta A \exp\left(-\frac{z}{d_0}\right) + \frac{1}{3}, \quad (6)$$

where ΔA represents the introduced distortion at the interface with respect to $\frac{1}{3}$, the ideal bulk value, and d_0 is a characteristic disorder length. Such a disorder profile has been successfully used in modeling Raman scattering data.⁷⁴ Further, by substituting for A the its spatial average \bar{A} with respect to the film thickness into Eq. (4) one obtains an analytical model for the thickness-dependent frequency shift observed experimentally. Fitting the ir measurements to Eq. (4) having assigned ΔA , d_0 , and e^* as fit parameters results in the typical curves presented in Figs. 13 and 14 for the SiH and SiH₂ vibrations, respectively. For the rest of the parameters entering Eq. (4) the values mentioned in Sec. IV A were taken. The excellent agreement with the experimental data for both SiH and SiH₂ groups is to be noted.

2. Determination of the effective dynamical charges

By fitting the experimentally determined frequency shifts to Eq. (4) it is possible to obtain an estimate of the effective dynamical charge of the vibrating dipole. Averaging the fit results on e^* for all substrates and temperatures studied gives the values 0.41 ± 0.01 and 0.24 ± 0.03 (in elemental charge units) for SiH and SiH₂ groups, respectively. These results are in very good agreement with those determined by other workers using different experimental methods (see Table II).

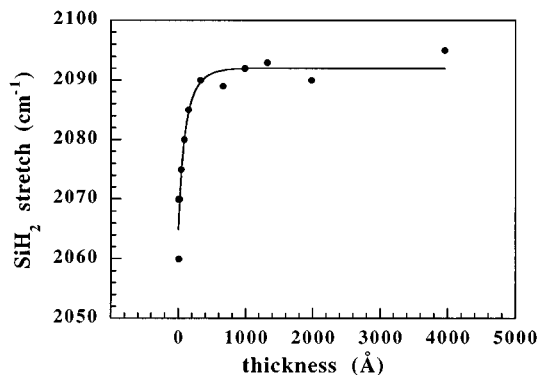


FIG. 14. Fit of the SiH₂-group vibrational frequency as a function of the film thickness for *a*-Si:H deposited on glass at 180 °C.

TABLE II. Effective dynamical charges (in elemental charge units) of the Si-H bond stretching vibration mode in SiH and SiH₂ groups in *a*-Si:H obtained from various references.

Reference	e^* (SiH)	e^* (SiH ₂)
5	0.80	0.24
84	0.39	
49	0.40	0.29
85	0.38	
76	0.44	0.26
32	0.39	0.26
75	0.44	0.44
This study	0.41	0.24

At this point, a brief discussion about the methods of determination of the effective charge and its nature seems to be necessary. The values of e^* given in Table II, except for ours and Cardona's, were determined by calibrating the ir absorption strengths of the Si-H stretching modes with the absolute H content in the samples measured by nuclear techniques. The unusually large value of e^* (SiH) reported by Shanks, Jeffrey, and Lowry⁵ was obtained under the assumption of independent H concentrations in the 2000- and 2100-cm⁻¹ modes, which, in general, does not hold. Cardona used the polarized medium model in order to explain the Si-H vibrational frequencies in *a*-Si:H and found that the effective charge reported in Table II agrees well with experiment. The method in the present study is based on the explanation of the thickness-dependent frequency shifts of the Si-H modes in terms of the polarized medium model and is, consequently, a modification of Cardona's method. Both groups of methods, the calibrated H-bond absorption and the polarized medium, give, except for the last reported SiH₂ value, consistent results on the SiH and SiH₂ effective charges. In a recent study, Daey Ouwens, Schropp, and van der Weg⁷⁵ assumed somewhat arbitrarily the equality of both SiH- and SiH₂-mode effective charges and obtained them to be equal to the *a*-Si dynamical charge, hence the above discrepancy. However, there is no theoretical evidence for considering both these charges as having identical values, moreover, a different value should be attributed to each Si-H vibrational mode.^{5,32,76} It should be noted that the value of the effective charge for 2100-cm⁻¹ vibration is often interpreted as a weighted average of the respective values for polyhydrides (SiH₂) and clustered monohydrides (SiH in microvoids).³² The proximity between the effective charge values independently determined by calibrated H-absorption method, on one hand, and by the polarized medium methods, on the other, clearly indicates the consistency of the latter.

3. Physical considerations

Although describing well the experimentally determined behavior of the Si-H vibrational frequency shift, the polarized medium model does not reveal the physical reasons for the thickness-dependent disorder in *a*-Si:H. Here we shall briefly discuss the possible physical phenomena leading to an increased interface disorder.

One possible picture is the deposition of microparticulates at the substrate surface at the very first stage of film deposi-

tion, as mentioned before. These inhomogeneities consist of clusters of several Si and H atoms that may be formed in the plasma discharge.⁷⁷ The temperature assisted diffusion of the depositing species, mainly the SiH₃ radical,⁵⁸ will not be able to entirely fill the gaps between the clusters and an interface layer morphologically different from the bulk material will be formed. However, it is established that the formation of clusters is typical of high-power decomposition of silane^{62,78} and therefore the presence of buried microparticulates in our low-power deposited films is quite unlikely. Moreover, these clusters are known to exhibit mostly a (SiH)_n-type structure,⁷⁷ which would leave unexplained the SiH₂ frequency behavior.

Increased interface disorder may also result from the incomplete coalescence of nuclei at the substrate surface during the growth, as already discussed. However, it is well known that nucleation does not occur on glass substrate, while interface disorder is obviously present on all substrates studied.

Energetic ion and neutral bombardment from the discharge may have a strong effect on the structure of the film surface. Bombardment-sputtered and redeposited radicals can cause poor film surface structure⁵⁸ and thereby increase the degree of disorder. The occurrence of significant bombardment-related effects is, however, very improbable under our deposition conditions, since the rf power used in the deposition process (50 mW/cm²) is too low. Thus Antoine *et al.*,⁷⁹ using an electrostatic analyzer technique, measured a very low ion flux (~2%) characterizing the ion bombardment under *a*-Si:H deposition conditions similar to ours.

A clue to the interface disorder may be searched in the reaction mechanisms at the growing film surface. In the very beginning of the deposition process the growth precursors (mainly the SiH₃ radical) arriving at the substrate surface start migrating in search of energetically favorable sites. However, in the initial stage of the surface growth the diffusion of the deposited species with high chemical reactivity is hindered because of the great number of dangling bonds and other surface defects. As a consequence, the interfacial structural randomness of the material achieves its maximum value. In extensive computer simulations of *a*-Si:H plasma deposition, Gleason *et al.*⁸⁰ revealed the presence of islands and lower lattice connectivity regions under the assumption of no species diffusion on the growing surface. In this way, the hindered migration of radicals results in the creation of a highly disordered and strained *a*-Si network. Furthermore, the above workers showed that the H concentration decreases as the diffusion radius is increased. Therefore, the smallest diffusion rate and, consequently, the highest degree of disorder should be observed at the film interface or surface, in agreement with the H accumulation at the film boundaries^{6,7} already mentioned. Later in the growth process, the bulk network achieves its highest possible degree of structural order and, as a consequence, the H concentration decreases. From spectroscopic point of view at this stage the Si-H bond vibrations achieve their "normal" bulk frequencies as can be seen, for example, in Figs. 2 and 3.

Note that the above species diffusion picture is supported by the temperature dependence of the characteristic disorder lengths, namely, their decrease with increasing temperature, as shown in Table III. This behavior is readily explained by

TABLE III. Characteristic disorder lengths d_0 for *a*-Si:H films deposited on Corning glass, Cr, and fused silica substrates at different deposition temperatures.

Substrate	Temperature (°C)	d_0 (Å)
Corning glass	110	1880
Corning glass	180	1242
Corning glass	250	548
Cr	180	1425
fused silica	180	~600

the increased diffusion radius with temperature. On the other hand, the dependence of the disorder lengths on the substrate nature (see Table III) can be qualitatively accounted for by the substrate-dependent sticking coefficients of *a*-Si:H film precursors leading to different surface mobilities, as suggested by Schmidt *et al.*⁶² Raman measurements on *a*-Si:H films also yield substrate-dependent disorder profiles with similar disorder lengths.²⁷ Finally, the insensitivity to doping (see Fig. 6) of the frequency shift effect is also easily explained in the frame of the disorder model, since it has been established using Raman scattering that the introduction of doping atoms into the *a*-Si:H network only weakly affects the short-range structural order (i.e., the order at the Si-tetrahedrons level).⁸¹

Although explaining well the substrate and temperature dependence of the frequency shifts, the above migration-diffusion picture is unable to account for the large characteristic disorder lengths for the SiH group; see Table III. Indeed, it is known that migration processes begin to stabilize after about several hundred angstroms at the most, while the disorder lengths observed suggest changes in the intermediate-range order (~10³ Å). The explanation for these results has to be sought in the structural role played by hydrogen in the *a*-Si:H network. Namely, the presence of H in high concentrations results in changes in the structural topology of *a*-Si:H given the univalent nature of H. This induces modifications of intermediate-range order and topology of the existing network through the alterations of the bond-length and bond-angle distributions of neighboring Si atoms.⁶⁵ Quantitatively, this phenomenon is described by the quasi-interstitial hydrogen model. This model, as proposed by Hishikawa *et al.*,⁴⁶ suggests that one of the roles of the H atom bonded in monohydride configuration (SiH) is to act as an interstitial impurity in the silicon network, yielding repulsive forces between itself and the neighboring Si atoms and thus introducing structural distortions. It is important to note that Raman scattering^{46,82} and stress measurements⁴⁶ supporting this model give disorder profiles similar to those determined by ir ellipsometry.

The above physical considerations clearly reveal the double role played by H in the *a*-Si:H structure, namely, by influencing the short-range order through favoring surface migration and diffusion, as well as the intermediate-range one by the H atom acting as an interstitial impurity leading to a distorted network.

It is essential to note the presence of two disorder length scales in *a*-Si:H as revealed by the ellipsometry measurements of the SiH and SiH₂ group vibrations (see Figs. 2 and 3). The first one, of the order of 10 Å, characterizes the

relaxation of the structural distortions in the ultrathin layer adjacent to the interface and is given by the SiH₂-group frequency behavior, since it is well known that a SiH₂ rich layer is formed at the film interface and surface during *a*-Si:H plasma deposition, as already noted. In the frame of the physical picture discussed above the structural relaxation at the interface is assisted by H bonded in dihydride configuration known to introduce structural flexibility in the Si network and reduce the stress in the films.⁴⁶ The second disorder length scale ($\sim 10^2$ – 10^3 Å) reflects the transition from surface to bulk material properties and is revealed by the SiH frequency behavior, since the SiH groups are homogeneously distributed in the bulk *a*-Si:H. At the atomic level, it evidences the role of monohydride-bonded H as a distortion-generating interstitial impurity in the amorphous network. As a conclusion, the bond-angle (and probably the bond-length) distortions responsible for the disorder in the *a*-Si network do not decay uniformly from the interface to the bulk, but rather exhibit an abrupt fall at the interface, followed by a gradual decrease into the bulk. It is essential to note that the particular disorder profile in plasma-deposited *a*-Si:H layers strongly depends on the deposition conditions used²⁷ as well as on such “parameters” as reactor geometry or plasma-ignition procedure and may be even absent, as shown by recent studies.⁸³

However, ellipsometric measurements alone cannot give any information about the exact location of the disordered layer. That is, since in ellipsometry the light beam probes the whole layer (provided it is weakly absorbing), as mentioned before, in general no distinction can be made between surface and interface contributions. Similarly, the results of most of the experimental Raman spectroscopy studies can be interpreted in terms of interface or, equivalently, surface disorder. Under certain experimental conditions, however, a clear identification becomes possible. For example, using a surface laser excitation, Raman scattering measurements revealed the presence of surface disorder in thick *a*-Si:H films.⁸² In our case, the monotonic decay of the disorder profile in Fig. 11 obtained by a surface (Ar) excitation clearly indicates that bond-angle distortions are present at the interface. Thus structural disorder appears to be a characteristic feature of the film-substrate interface rather than of the film surface. This statement is supported by the above reaction model, as well as by the good agreement between the disorder characteristic lengths determined in our study and those found by Raman measurements on thin *a*-Si:H films²⁷ as well as on *a*-Si:H/*a*-SiN_x superlattices⁶⁸ where an interface-disorder effect has been unambiguously revealed. Moreover, the substrate dependence of the characteristic lengths (see Fig. 4) corroborates this picture too. A small

contribution of the surface cannot be entirely excluded, however. This may probably be the case of the SiH₂-group stretching vibration.

V. SUMMARY AND CONCLUSION

We have systematically studied the thickness dependence of the low-frequency shift of the Si-H stretching vibration of SiH and SiH₂ groups in *a*-Si:H thin films using ir ellipsometry. This effect was shown to depend on the substrate nature and the deposition temperature of the plasma-deposited *a*-Si:H. A review of possible physical explanations of the shift phenomenon accompanied by detailed discussions (such as the presence of substrate contaminants and the defect state profile) has been made. Finally, the bond-angle disorder of the *a*-Si:H network at the film-substrate interface was shown to be responsible for the vibrational frequency shifts. A physical picture of the film-growth mechanisms leading to an increased interface disorder and the role of hydrogen played in it was discussed. Analytical modeling of the experimental results using the polarized medium model allowed us to obtain the effective charge of the Si-H bond in different configurations (SiH and SiH₂). The values of the effective charges thus obtained are $(0.41 \pm 0.01)e$ and $(0.24 \pm 0.03)e$ (where e denotes the elemental charge) for the SiH and SiH₂ group vibrations, respectively. The above results are in very good agreement with those of ir absorption and Raman scattering studies. More generally, the influence of the structural properties (e.g., bond-angle disorder) on the vibrational properties is evidenced, physically explained, and analytically modeled. Thus ir spectroscopy techniques (ir ellipsometry, in particular) are shown to be able to indirectly monitor network-disorder effects through the influence of the latter on the vibrational properties of thin-film materials, in a similar way as Raman scattering spectroscopy, which is generally considered to give direct results on changes in local structural order.

ACKNOWLEDGMENTS

We are grateful to Dr. M. Favre, Dr. P. Roca i Cabarrocas, Dr. R. Darwich, and Dr. J. Perrin for helpful discussions on the defect density profile and intrinsic stress in *a*-Si:H as well as on the polarization theory. Dr. H. Shirai's help in fitting some of the spectral lines considerably facilitated the analysis of the results. We are indebted to the staff of the Raman Laboratory of ISA Jobin-Yvon and, in particular, to Dr. M. Stchakovsky for having performed the Raman scattering measurements. We would like to express our gratitude to Dr. P. Morin for his assistance.

*Present address: ISA Jobin-Yvon, 16-18 rue du Canal, 91165 Longjumeau, France.

¹M. H. Brodsky, M. Cardona, and J. J. Cuomo, *Phys. Rev. B* **16**, 3556 (1977).

²G. Lucovsky, R. J. Nemanich, and J. C. Knights, *Phys. Rev. B* **19**, 2064 (1979).

³W. Paul, *Solid State Commun.* **34**, 283 (1980).

⁴H. Wagner and W. Beyer, *Solid State Commun.* **48**, 585 (1983).

⁵H. R. Shanks, F. R. Jeffrey, and M. E. Lowry, *J. Phys. (Paris) Collog.* **42**, C4-773 (1981).

⁶Y. Toyoshima, K. Arai, A. Matsuda, and K. Tanaka, *Appl. Phys. Lett.* **57**, 1028 (1990).

⁷N. Blayo and B. Dréville, *J. Non-Cryst. Solids* **137&138**, 771 (1991).

⁸M. Katiyar, G. F. Feng, J. R. Abelson, and N. Maley, in *Amorphous Silicon Technology—1991*, edited by A. Madan *et al.*,

- MRS Symposia Proceedings No. 219 (Materials Research Society, Pittsburgh, 1991), p. 295.
- ⁹Y. Toyoshima, K. Arai, A. Matsuda, and K. Tanaka, *J. Non-Cryst. Solids* **137&138**, 765 (1991).
- ¹⁰N. Blayo, P. Blom, and B. Drévilion, *Physica B* **170**, 566 (1991).
- ¹¹B. Drévilion, *Prog. Cryst. Growth Charact.* **27**, 1 (1993).
- ¹²A. M. Antoine, B. Drévilion, and P. Roca i Cabarrocas, *J. Appl. Phys.* **61**, 2501 (1987).
- ¹³N. Blayo, B. Drévilion, and R. Ossikovski, in *Optically Based Methods for Process Analysis*, edited by D. S. Bromse *et al.* [SPIE Symp. Proc. **1681**, 116 (1992)].
- ¹⁴M. J. Dignam, B. Rao, M. Moskovits, and R. W. Stobie, *Can. J. Appl. Chem.* **49**, 1115 (1971).
- ¹⁵R. Ossikovski, B. Drévilion, and J. Perrin, *J. Non-Cryst. Solids* **164–166**, 107 (1993).
- ¹⁶M. K. Gunde and B. Aleksandrov, *Appl. Spectrosc.* **44**, 970 (1990).
- ¹⁷W. R. Knolle and D. L. Allara, *Appl. Spectrosc.* **40**, 1046 (1986).
- ¹⁸M. K. Gunde, *Appl. Spectrosc.* **46**, 365 (1992).
- ¹⁹R. Ossikovski, B. Drévilion, and M. Firon, *J. Opt. Soc. Am. A* **12**, 1797 (1995).
- ²⁰H. Piller, in *Handbook of Optical Constants of Solids*, edited by E. Palik (Academic, Orlando, 1985), p. 571.
- ²¹D. W. Lynch and W. R. Hunter, in *Handbook of Optical Constants of Solids II*, edited by E. Palik (Academic, San Diego, 1991), p. 374; D. F. Edwards, in *Handbook of Optical Constants of Solids* (Ref. 20), p. 547.
- ²²M. A. Baker, *Thin Solid Films* **69**, 359 (1980).
- ²³N. Blayo and B. Drévilion, *Appl. Phys. Lett.* **57**, 786 (1990).
- ²⁴G. Lucovsky, *Solid State Commun.* **29**, 571 (1979).
- ²⁵D. V. Tsu, G. Lucovsky, and B. N. Davidson, *Phys. Rev. B* **40**, 1795 (1989).
- ²⁶T. S. Shi, S. N. Sahu, G. S. Oehrlein, A. Hiraki, and J. W. Corbett, *Phys. Status Solidi A* **74**, 329 (1982).
- ²⁷Y. Hishikawa, S. Tsuge, N. Nakamura, S. Tsuda, S. Nakano, and Y. Kuwano, *Appl. Phys. Lett.* **57**, 771 (1990).
- ²⁸D. V. Tsu and G. Lucovsky, *J. Non-Cryst. Solids* **97&98**, 839 (1987).
- ²⁹R. Street, *Hydrogenated Amorphous Silicon* (Cambridge University Press, Cambridge, 1991), pp. 20 and 35.
- ³⁰M. Favre, H. Curtins, and A. V. Shah, *J. Non-Cryst. Solids* **97&98**, 731 (1987).
- ³¹J. P. Kleider, C. Longeaud, and P. Roca i Cabarrocas, *J. Appl. Phys.* **72**, 4727 (1992).
- ³²A. A. Langford, M. L. Fleet, B. P. Nelson, W. A. Lanford, and N. Maley, *Phys. Rev. B* **45**, 13 367 (1992).
- ³³S. Oguz, D. A. Anderson, W. Paul, and H. J. Stein, *Phys. Rev. B* **22**, 880 (1980).
- ³⁴O. Grimal, D. P. Masson, L. Bertrand, and A. Yelon, *Phys. Rev. B* **49**, 10 242 (1994).
- ³⁵D. Bermejo and M. Cardona, *J. Non-Cryst. Solids* **32**, 405 (1979).
- ³⁶B. Bech Nielsen and H. G. Grimmeis, *Phys. Rev. B* **40**, 12 403 (1989).
- ³⁷Y. J. Chabal and K. Raghavachari, *Phys. Rev. Lett.* **34**, 1055 (1985).
- ³⁸Y. Okada and S. Nakajima, *Appl. Phys. Lett.* **59**, 1066 (1991).
- ³⁹M. A. El Khakani, M. Chaker, A. Jean, S. Boily, H. Pépin, J. C. Kieffer, and S. C. Gujrathi, *J. Appl. Phys.* **74**, 2834 (1993).
- ⁴⁰J. P. Harbisson, A. J. Williams, and D. V. Lang, *J. Appl. Phys.* **55**, 946 (1983).
- ⁴¹T. I. Kamins and K. L. Chiang, *J. Electrochem. Soc.* **129**, 2331 (1982).
- ⁴²J. C. Phillips, *Phys. Rev. Lett.* **42**, 1151 (1979).
- ⁴³P. Paduschek, C. Höpfl, and H. Mitlehner, *Thin Solid Films* **110**, 291 (1983).
- ⁴⁴H. Windischmann, R. W. Collins, and J. M. Cavese, *J. Non-Cryst. Solids* **85**, 261 (1986).
- ⁴⁵K. Ozawa, N. Takagi, and K. Asama, *Jpn. J. Appl. Phys.* **22**, 767 (1983).
- ⁴⁶Y. Hishikawa, K. Watanabe, S. Tsuda, S. Nakano, M. Ohnishi, and Y. Kuwano, *J. Non-Cryst. Solids* **97&98**, 399 (1987).
- ⁴⁷H. Wieder, M. Cardona, and C. R. Guarnieri, *Phys. Status Solidi B* **92**, 99 (1979).
- ⁴⁸H. Shanks, C. J. Fang, L. Ley, M. Cardona, F. J. Demond, and S. Kalbitzer, *Phys. Status Solidi B* **100**, 43 (1980).
- ⁴⁹M. Cardona, *Phys. Status Solidi B* **118**, 463 (1983).
- ⁵⁰L. Onsager, *J. Am. Chem. Soc.* **58**, 1486 (1936).
- ⁵¹E. Bauer and M. Magat, *J. Phys. (Paris)* **9**, 319 (1938).
- ⁵²Z. Jing, J. L. Whitten, and G. Lucovsky, *Phys. Rev. B* **45**, 13 978 (1992).
- ⁵³M. H. Brodsky and D. Kaplan, *J. Non-Cryst. Solids* **32**, 431 (1979).
- ⁵⁴A. H. Mahan, D. L. Williamson, B. P. Nelson, and R. S. Crandall, *Phys. Rev. B* **40**, 12 024 (1989).
- ⁵⁵J. Powling and H. J. Bernstein, *J. Am. Chem. Soc.* **73**, 1815 (1951).
- ⁵⁶A. D. E. Pullin, *Spectrochim. Acta* **13**, 125 (1958).
- ⁵⁷A. Takano, M. Kawasaki, and H. Koinuma, *J. Appl. Phys.* **73**, 7987 (1993).
- ⁵⁸A. Gallagher and J. Scott, *Solar Cells* **21**, 147 (1987).
- ⁵⁹R. W. Collins, in *Advances in Disordered Semiconductors*, edited by H. Fritzsche (World Scientific, Singapore, 1989), Vol. B, p. 1003.
- ⁶⁰A. Canillas, E. Bertran, J. L. Andújar, and B. Drévilion, *J. Appl. Phys.* **68**, 2752 (1990).
- ⁶¹A. M. Antoine and B. Drévilion, *J. Appl. Phys.* **63**, 360 (1988).
- ⁶²U. I. Schmidt, W. Herbst, B. Schröder, and H. Oechsner, in *Amorphous Silicon Technology—1994*, edited by E. A. Schiff *et al.*, MRS Symposium Proceedings No. 336 (Materials Research Society, Pittsburgh, 1994), p. 85.
- ⁶³K. Winer and M. Cardona, *Solid State Commun.* **60**, 207 (1986).
- ⁶⁴L. Ley, J. Reichardt, and R. L. Johnson, *Phys. Rev. Lett.* **49**, 1664 (1982).
- ⁶⁵N. Maley and J. S. Lannin, *Phys. Rev. B* **36**, 1146 (1987).
- ⁶⁶J. S. Lannin, L. J. Pilione, S. T. Kshirsagar, R. Messier, and R. C. Ross, *Phys. Rev. B* **26**, 3506 (1982).
- ⁶⁷N. Maley and J. S. Lannin, *Phys. Rev. B* **31**, 5577 (1985).
- ⁶⁸I. Honma, T. Tanaka, H. Komiyama, and K. Tanaka, in *Amorphous Silicon Technology—1989*, edited by A. Madan, MRS Symposium Proceedings No. 149 (Materials Research Society, Pittsburgh, 1989), p. 669.
- ⁶⁹H. J. Stein and P. S. Peercy, *Phys. Rev. B* **22**, 6233 (1980).
- ⁷⁰Y. J. Chabal, G. S. Higashi, and S. B. Christman, *Phys. Rev. B* **28**, 4472 (1983).
- ⁷¹Y. J. Chabal, *Phys. Rev. Lett.* **23**, 1850 (1983).
- ⁷²C. J. F. Böttcher, *Theory of Electric Polarization* (Elsevier, Amsterdam, 1973), Vol. 1, pp. 138, 88, and 149.
- ⁷³S. Berthier, *Optique des Milieux Composites* (Polytechnica, Paris, 1993), p. 191.
- ⁷⁴N. Maley and J. S. Lannin, *J. Non-Cryst. Solids* **77&78**, 1073 (1985).

- ⁷⁵J. Daey Ouwens, R. E. I. Schropp, and W. F. van der Weg, *Appl. Phys. Lett.* **65**, 204 (1994).
- ⁷⁶G. Amato, G. Della Mea, F. Fizzotti, C. Manfredotti, R. Marchisio, and A. Paccagnella, *Phys. Rev. B* **43**, 6627 (1991).
- ⁷⁷T. P. Martin and H. Schaber, *J. Chem. Phys.* **83**, 855 (1985).
- ⁷⁸H. Shirai, B. Dré villon, N. Layadi, and P. Roca i Cabarrocas, *J. Non-Cryst. Solids* **164–166**, 119 (1993).
- ⁷⁹A. M. Antoine, B. Dré villon, and P. Roca i Cabarrocas, *J. Appl. Phys.* **61**, 2501 (1987).
- ⁸⁰K. K. Gleason, K. S. Wang, M. K. Chen, and J. A. Reimer, *J. Appl. Phys.* **61**, 2866 (1987).
- ⁸¹A. P. Sokolov, A. P. Shebanin, O. A. Golikova, and M. M. Mezdrogina, *J. Non-Cryst. Solids* **137&138**, 99 (1991).
- ⁸²G. Morell, R. S. Katiyar, S. Z. Weisz, M. Gomez, and I. Balberg, in *Amorphous Silicon Technology—1993*, edited by E. A. Schiff *et al.*, MRS Symposium Proceedings No. 297 (Materials Research Society, Pittsburgh, 1993), p. 321.
- ⁸³A. J. M. Berntsen, W. G. J. H. M. van Sark, and W. F. van der Weg, *J. Appl. Phys.* **78**, 1964 (1995).
- ⁸⁴G. Lucovsky, J. Yang, S. S. Chao, J. E. Tyler, and W. Czubatyi, *Phys. Rev. B* **28**, 3225 (1983).
- ⁸⁵N. Blayo and B. Dré villon, *Appl. Phys. Lett.* **52**, 950 (1991).